SCIENTIFIC REPORTS

OPEN

SUBJECT AREAS:
ELECTRONIC PROPERTIES AND DEVICES
CHEMICAL PHYSICS
GRAPHENE
COMPUTATIONAL CHEMISTRY

Received
22 March 2013

Accepted
23 May 2013

Published
19 June 2013

Correspondence and requests for materials should be addressed to Z.C. (zhongfangchen@gmail.com)

Preserving the Edge Magnetism of Zigzag Graphene Nanoribbons by Ethylene Termination: Insight by Clar's Rule

Yafei Li[1], Zhen Zhou[2], Carlos R. Cabrera[1] & Zhongfang Chen[1]

[1]Department of Chemistry, Institute for Functional Nanomaterials, NASA-URC Center for Advanced Nanoscale Materials, University of Puerto Rico, Rio Piedras Campus, San Juan, PR 00931, [2]Computational Centre for Molecular Science, Key Laboratory of Advanced Energy Materials Chemistry (Ministry of Education), Institute of New Energy Material Chemistry, Nankai University, Tianjin 300071, China.

By means of density functional theory computations, we demonstrated that C_2H_4 is the ideal terminal group for zigzag graphene nanoribbons (*z*GNRs) in terms of preserving the edge magnetism with experimental feasibility. The C_2H_4 terminated *z*GNRs (C_2H_4-zGNRs) with pure sp^2 coordinated edges can be stabilized at rather mild experimental conditions, and meanwhile reproduce the electronic and magnetic properties of those hydrogen terminated *z*GNRs. Interestingly, the electronic structures and relative stability of C_2H_4-*z*GNRs with different edge configurations can be well interpreted by employing the Clar's rule. The multiple edge hyperconjugation interactions are responsible for the enhanced stability of the sp^2 coordinated edges of C_2H_4-zGNRs. Moreover, we demonstrated that even pure sp^2 termination is not a guarantee for edge magnetism, for example, C_2H_2 termination can couple to the π-electron system of *z*GNRs, and destroy the magnetism. Our studies would pave the way for the application of *z*GNRs in spintronics.

Since its experimental realization in 2004[1,2], graphene, the first strict two-dimensional (2D) crystal with one-atomic thickness, has been a subject of great interest due to its excellent properties and promising applications[3–5]. Interestingly, one dimensional (1D) graphene nanoribbons (GNRs) can also be yielded by cutting graphene in the nano-scaled width. Depending on the cutting direction, two unique types of edges can be obtained: zigzag and armchair. Different from graphene which is actually semimetal, both zigzag and armchair GNRs have a nonzero band gap, which has been confirmed both theoretically[6,7] and experimentally[8,9]. Moreover, the edge geometry also makes a huge difference in the π-electron structure at the edges. As early as in 1996, Fujita *et al.*[10] revealed that zigzag GNRs (*z*GNRs) have peculiar localized edge states (completely absent in the armchair edge), which give rise to the quite flat bands near the Fermi level[11]. By employing the Hubbard model with the unrestricted Hartree-Fock approximation, Fujita *et al.*[10,12] also deduced that the edge states of *z*GNRs are ferromagnetically (FM) coupled on each edge but antiferromagnetically (AFM) coupled between two edges. In 2006, Son *et al.*[13] found that the edge states of *z*GNRs in different spin channels response oppositely to the transverse external electric field, and thus *z*GNRs can be half-metallic (metallic for one spin channel and insulating for the other) under a critical value of electric field. Later theoretical studies demonstrated that selective edge modification[14,15] can also tune *z*GNRs into half-metallic. Therefore, *z*GNRs have very promising applications in future spintronics.

However, there is a large gap between theoretical prediction and experimental realization. The edge states of zGNRs are very reactive[16], and thus cause instability, whereas armchair edges are more stable[17–19]. As a consequence, most synthesized nanographenes have armchair peripheries[20,21], and the synthesis of GNRs with consecutive zigzag edges has been rather difficult for a long time. Encouragingly, experimental peers have achieved great progress recently in fabricating GNRs with smooth zigzag edges[22–26], and the localized edge states have been vigorously confirmed by scanning tunneling microscopy (STM) and spectroscopy[27–31]. However, the edge magnetism of *z*GNRs has been scarcely detected experimentally[32,33], because, to preserve the edge magnetism, the edge sites of *z*GNRs should have the pure sp^2 coordination. Unfortunately, density functional theory

(DFT) computations by Wassmann *et al.*[34] demonstrated that the pure sp^2 coordinated edges of hydrogen terminated *z*GNRs (H-*z*GNRs) can be stabilized only at extremely low hydrogen concentration, which is rather challenging experimentally. Under normal conditions, the edge sites tend to be fully saturated by hydrogen, which directly suppresses the edge magnetism. More seriously, *z*GNRs are also characterized by the nonmagnetic nature in presence of some typical atmospheric molecules, such as O_2, H_2O, NH_3, and CO_2[35].

Therefore, to preserve the edge magnetism of *z*GNRs, the first urgent thing is to find a suitable termination group for *z*GNRs. Recently, Chai *et al.*[36] have suggested that large bulky ligands (i.e. tertiary-butyl, C_4H_9) terminated *z*GNRs favor the pure sp^2 termination across a broader range of thermodynamic conditions due to the strong steric effect of ligands. Though not mentioned explicitly, the hyperconjugation between the large bulky ligands and the edge states (can be seen as radicals)[16,37] also contributes to the enhanced stability of the edge. Then, an interesting question arises: can we use some more simple terminal groups to stabilize sp^2 coordinated edges of *z*GNRs by taking advantage of hyperconjugation interaction?

In this work, by means of systematic DFT computations, we explored the possibility of using ethylene (C_2H_4), a very simple and common organic molecule, as the terminal group for *z*GNRs to preserve the edge magnetism. C_2H_4 was chosen due to two reasons: (1) experimentally C_2H_4 is an important carbon resource for graphene growth[38,39], and thus technically it would be rather practical to use C_2H_4 as terminal group for *z*GNRs; (2) after bonding to edges sites, the C–H bonds of C_2H_4 can have hyperconjugation interaction with edge states. Our computations demonstrated that due to the multiple edge hyperconjugation interactions, sp^2 coordinated edges of C_2H_4 terminated *z*GNRs (C_2H_4-*z*GNRs) can be realized at rather mild experimental conditions, and C_2H_4-*z*GNRs can well reproduce the electronic and magnetic properties of H-*z*GNRs.

Results

To ascertain whether the edge magnetism of *z*GRNs can be preserved by C_2H_4 termination, we need to determine the most stable edge configuration for C_2H_4-*z*GNRs firstly. In our computations, C_2H_4-*z*GNR with a width parameter of 8 (8-C_2H_4-*z*GNR) was chosen as a representative (Figure 1). For simplicity, two edges of 8-C_2H_4-*z*GNR were set to have the same configuration. Following the previous convention[34–36], the edge configurations are denoted with $z_{n_1 n_2 \ldots n_x}$, where $n_i = 1, 2$ stands for the number of C_2H_4 molecules bonded to the *i*th edge site, and *x* is the number of edge sites in a unit cell. Six edge configurations, including z_{11}, z_{121}, z_{11121}, z_{22}, z_{1122}, and z_{111122} were considered. Here note that different from H, one C_2H_4 can bond to two edge sites, thus some edge configurations consisting of odd number of sp^2 edge sites, such as z_{12} and z_{1112}, are only available for H termination but not available for C_2H_4 termination. Moreover, we also considered the reconstructed zigzag edge, in which two hexagons transform into a pentagon and a heptagon, denoted as $z(57)$[19]. This haeckelite edge structure has been observed experimentally[40]. For $z(57)$, two possible edge configurations, including $z(57)_{11}$ and $z(57)_{22}$, were investigated.

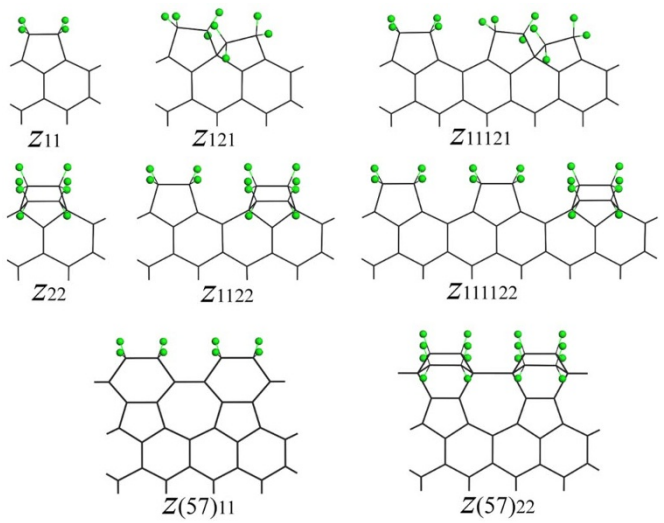

Figure 1 | Schematic structures of edge configurations for 8-C_2H_4-*z*GNR. Black line and green ball represent carbon and hydrogen, respectively.

To compare the stability of these edge configurations, we first computed the edge formation energy (E_{edge}) for each configuration, which is defined as:

$$E_{edge} = \frac{1}{2L}\left(E_{ribbon} - (N_C - 2N_{C_2H_4})E_{graphene} - N_{C_2H_4}E_{C_2H_4}\right) \quad (1)$$

where E_{ribbon}, $E_{graphene}$, and $E_{C_2H_4}$ are the total energies of the nanoribbon, one carbon atom of graphene, and one C_2H_4 molecule, respectively. N_C and $N_{C_2H_4}$ are the numbers of carbon atoms and C_2H_4 groups in the supercell, respectively. *L* is the length of one unit cell. According to this definition, the edge configurations with lower E_{edge} values are more favorable energetically at 0 K. For comparison, the E_{edge} of 8-H-*z*GNR with pure sp^2 termination ($z(H)_1$) was also computed. The computed E_{edge} of all the considered edge configurations and their corresponding ground states are summarized in Table 1. According to our computations, for C_2H_4-*z*GNRs, the nonmagnetic edge configuration z_{111122} has the lowest value of E_{edge}, tightly followed by the pure sp^2 coordinated edge configuration z_{11}. Especially, the E_{edge} of z_{11} is lower than $z(H)_1$, implying that C_2H_4 termination could produce more stable sp^2 coordinated edge than hydrogen termination.

However, the content of C_2H_4 changes under real experimental conditions, and the chemical potential of C_2H_4 should be taken into account. Thus, we evaluated the relative stability of different edge configurations for 8-C_2H_4-*z*GNR under real experimental conditions by comparing their respective Gibbs formation energy (ΔG_{edge}), which is defined as:

$$\Delta G_{edge} = E_{edge} - \frac{N_{C_2H_4}}{2L}\mu_{C_2H_4} \quad (2)$$

where $\mu_{C_2H_4}$ is a function of the temperature *T* and the partial C_2H_4 gas pressure *P*, and can be expressed as:

$$\mu_{C_2H_4} = H^o(T) - H^o(0) - TS^o(T) + k_B T \ln\left(\frac{P}{P^o}\right) \quad (3)$$

H^o and S^o are the enthalpy and entropy at the pressure $P^o = 1$ bar, respectively, the values of which at T = 298 K are obtained from the

Table 1 | Edge formation energy (E_{edge}) for all the considered edge configurations of C_2H_4-terminated 8-*z*GNRs and their corresponding ground states (GS). The corresponding values for the z_1 configuration of H-terminated 8-*z*GNRs are given for comparison

	E_{edge} (eV/Å)	GS
z_{11}	0.0096	magnetic
z_{121}	0.0257	nonmagnetic
z_{11121}	0.0145	nonmagnetic
z_{1122}	0.0170	nonmagnetic
z_{111122}	0.0020	nonmagnetic
z_{22}	0.2240	magnetic
$z(57)_{11}$	0.4252	nonmagnetic
$z(57)_{22}$	0.4401	nonmagnetic
$z(H)_1$	0.0676	magnetic

textbook[41]. Then, we plotted the curve of ΔG_{edge} for 8-C_2H_4-zGNR with different edge configurations as a function of $\mu_{C_2H_4}$ in Figure 2. According to the above definition, the most stable edge configuration should have the lowest value of ΔG_{edge} within a given value of $\mu_{C_2H_4}$.

Several conclusions can be drawn from Figure 2. First, the ΔG_{edge} of z_{121}, z_{11121}, $z(57)_{11}$, or $z(57)_{22}$ could never be the lowest at any given value of $\mu_{C_2H_4}$, indicating that these four edge configurations have no chance to be realized under real experimental conditions. Especially, the unfavorability of $z(57)_{11}$ and $z(57)_{22}$ suggests that the reconstruction of zigzag edge can be suppressed under the C_2H_4 environment. Second, the ΔG_{edge} of z_{22} is the lowest when $\mu_{C_2H_4}$ is larger than 2.03 eV, indicating that z_{22} can be stabilized only at extremely high C_2H_4 concentration. When $\mu_{C_2H_4}$ is in the range of [0.44, 2.03] eV, z_{1122} becomes stable. z_{111122}, which has the lowest value of E_{edge}, is stable only in a rather narrow range of [−0.11, 0.44]. When $\mu_{C_2H_4} < -0.11$ eV, z_{11} becomes the most stable edge configuration. At room temperature, −0.11 eV of $\mu_{C_2H_4}$ corresponds to a C_2H_4 pressure (P) of 2.45 bar. In other words, if the C_2H_4 pressure can be controlled to be lower than 2.45 bar at room temperature, which is experimentally rather feasible, the pure sp^2 coordinated edges can be stabilized. In sharp contrast, pure sp^2 coordinated edges of H-zGNRs can be stabilized only at extremely low hydrogen concentration and thus unlikely to be realized. Therefore, C_2H_4 is superior to hydrogen as a terminal group for zGNRs in terms of generating pure sp^2 coordinated edges and preserving the edge magnetism. Experimentally, C_2H_4-zGNRs can be synthesized via lithographic patterning of graphene under the C_2H_4 atmosphere, or by etching the edges of pre-obtained zGNRs using C_2H_4 gas.

After establishing that pure sp^2 coordinated edges of zGNRs, namely, z_{11}, can be produced by C_2H_4 termination at mild experimental conditions, we quite wonder the magnetic and electronic properties of C_2H_4-zGNRs with z_{11} edge configuration. The same as H-zGNRs, our computations also revealed an AFM ground state for C_2H_4-8-zGNRs, which is 2 and 24 meV/edge atom lower in energy than the FM and NM states, respectively. For comparison, the AFM state of 8-H-zGNR is 2 and 26 meV/edge atom lower in energy than the FM and NM states, respectively.

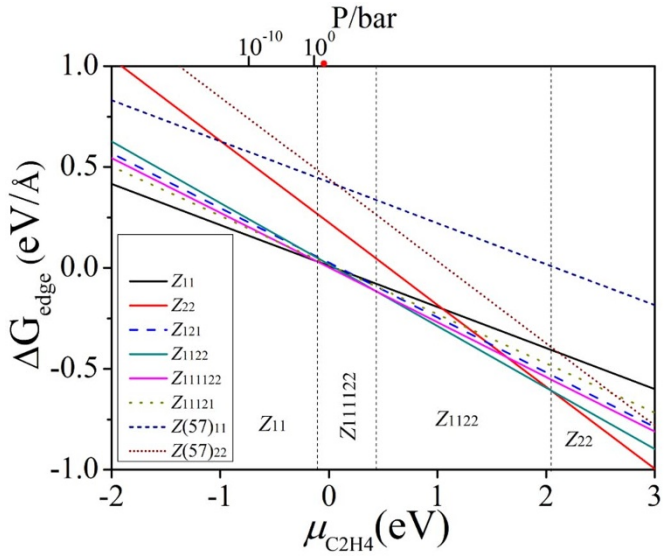

Figure 2 | Gibbs formation energy (ΔG_{edge}) as a function of chemical potential ($\mu_{C_2H_4}$) for different edge configurations of 8-C_2H_4-zGNR. The solid lines denote the stable edge configurations under certain $\mu_{C_2H_4}$ values. Vertical dashed lines divide the stability regions. The upper axis shows the pressure of C_2H_4, corresponding to the chemical potential at 298 K. The red dot denotes the position of saturated vapor pressure of C_2H_4 at 298 K.

Figure 3a presents the spatial distribution of the charge difference between α-spin and β-spin for 8-C_2H_4-zGNR. The magnetization per edge atom of C_2H_4-8-zGNR is 0.13 μB (0.15 μB for 8-H-zGNR), decaying gradually from two edges to the inner. Therefore, the stability and magnitude of edge magnetism of C_2H_4-zGNRs are comparable to those of H-zGNRs.

Then, we computed the band structure of 8-C_2H_4-zGNR in the AFM state. As shown in Figure 3b, 8-C_2H_4-zGNR has a 0.42 eV (0.45 eV for 8-H-zGNR) band gap for both spin channels. Especially, the spin-polarized π and π^* bands are also quite flat near the Fermi level, a known symbol of edge states.

In lights of the above results, we conclude that C_2H-zGNRs can well reproduce the electronic and magnetic properties of those H-zGNRs. Therefore, C_2H_4-zGNRs may realize many fancy properties previously predicted for H-zGNRs, such as half-metallicity[13]. Our computations demonstrated that under a 0.7 V/Å transverse electric field, 8-C_2H-zGNR with z_{11} edge configuration can be tuned into half-metallic. Here note that generalized gradient approximation (GGA) usually predicts a much higher critical value of electric filed than local density approximation (LDA)[42].

Discussion

Although we have determined that pure sp^2 coordinated edges of zGNRs, namely, z_{11}, can be produced by C_2H_4 termination at rather mild experimental conditions, there is an obvious question to be explained: why does z_{121} have a relatively large value of E_{edge} and is unfavorable on the whole range of thermodynamics conditions? As revealed by Wassmann *et al.*[34], z_{121} has the lowest value of E_{edge} among all the edge configurations of H-zGNRs, and is stable in a rather boarder range of thermodynamic conditions. Then, what makes the difference for C_2H_4 and hydrogen terminations? Actually this difference is simply due to the steric effect of C_2H_4 molecules. As shown in Figure 1, in a unit cell of z_{121}, two C_2H_4 molecules bond to an edge site of zGNR together to generate a sp^3 edge site, and the rest two carbon atoms of C_2H_4 molecules bond to two edge sites of zGNR to generate two sp^2 edge sites. Due to the strong steric effect, two C_2H_4 molecules are pushed up and down, respectively, at the sp^3 edge sites. Thus, the strain imposed on two sp^2 edge sites causes a serious edge distortion (Figure S1 of supplementary information) and consequently increases the E_{edge}. Here note that for z_{111122} and z_{1122}, in which continuous two sp^3 coordinated edge sites are present, the edge distortion is absent. Since z_{121} has the same C_2H_4 density ($\frac{N_{C_2H_4}}{2L}$) as z_{111122} but a higher E_{edge} than z_{111122}, z_{121} could never be the most stable edge configuration in any given value of $\mu_{C_2H_4}$ according to equation (2), and is hence excluded from the phase diagram.

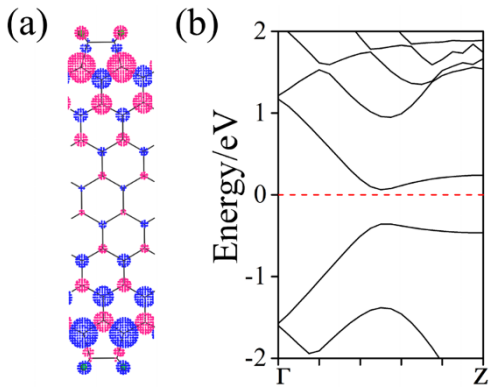

Figure 3 | Electronic structures of C_2H_4-zGNR. (a) Spatial distribution of the charge difference between α-spin (blue) and β-spin (red) and (b) band structure for 8-C_2H_4-zGNR with z_{11} edge configuration. The red dashed line denotes the position of Fermi level.

Besides the unstability problem of z_{121}, there are still some concerns to be addressed. For example, for these stable edge configurations on the whole range of thermodynamic conditions, why are z_{11} and z_{22} magnetic while $z_{1111122}$ and z_{1122} are nonmagnetic? Moreover, why does z_{11} have a rather low E_{edge}, while z_{22} has a higher E_{edge} than other stable edge configurations? Why does z_{111122} has an even lower E_{edge} than z_{11}?

The above concerns can be satisfactorily understood by the Clar's rule[43,44], which has been successfully applied for accounting the π electron distribution and reactivity of polycyclic aromatic hydrocarbons (PAH)[45–47] and many carbon nanomaterials[48–53]. According to the Clar's rule, the sp^2 coordinated carbon atoms of a close-shell PAH can be formulated into two structural units that are linked by single bonds, benzenoid aromatic ring and olefinic double bond, wherever necessary. A PAH is the most stable when it has the greatest number of benzenoid rings. The unusual stability of graphene can be understood as all carbon atoms are benzenoid with a maxima density of benzenoid rings of 1/3. Without considering the steric effect of termination groups (as for H-terminated zGNRs), z_{121} should be the most stable edge configuration for zGNRs since it enables that *z*GNRs have the same density of benzenoid rings as graphene (Figure S2 of supplementary information). However, for C_2H_4-terminated *z*GNRs, the enhanced stabilization from aromaticity is overwhelmed by the steric effect; thus the z_{121} configuration is not favored anymore.

For zGNRs with density of benzenoid rings lower than 1/3, there is a competition between maximizing the density of benzenoid rings for the bulk and imposing unsaturated carbon atoms on the edges. Taking z_{11} of 8-C_2H_4-zGNR as an example, if we assume that all its carbon atoms are saturated with four chemical bonds with neighboring atoms, z_{11} will form the quinonoid structure with two double bonds in each hexagon (Figure S3 of supplementary information), and the formation of benzenoid ring in z_{11} is completely forbidden. However, the quinonoid structure is quite unstable. In this case, z_{11} would impose two unpaired electrons on each edge in a 1×1×3 supercell, and the resulted nanoribbon has the same density of benzenoid rings (1/3) as graphene (Figure 4a). The energy gain from the resonance favors this electronic structure as the ground state. Therefore, z_{11} has a magnetic ground state with unpaired electrons on the edges. Moreover, the unpaired electrons of z_{11} have subtle hyperconjugation interactions with neighboring C=C bonds and C–H bonds of C_2H_4, which could stabilize the unpaired electrons (thus stabilizing the edge). Besides, there is also hyperconjugation interaction between C=C bonds and C–H bonds, which could also contribute to the stability of the edge. Thus, the multiple hyperconjugation interactions on the edge should be responsible for the rather favorable E_{edge} of z_{11}. In contrast, in H-*z*GNRs, there only exists the hyperconjugation interaction between unpaired electrons and C=C bonds, resulting in a larger E_{edge} for $z(H)_1$ than z_{11}.

Similarly, by imposing four unpaired electrons to the outer sp^2 carbon atoms on each edge in a 1×1×3 supercell, the interior carbon atoms of z_{22} can also maximize the density of benzenoid rings (Figure 4b). In contrast to z_{11}, only half of the unpaired electrons of z_{22} can have hyperconjugation interaction with C=C double bonds while the rest are localized. Such densely localized unpaired electrons on the edges result in a very high E_{edge} for z_{22}. These analyses can also explain why the magnetization of fully saturated edges of zGNRs is larger than the sp^2 coordinated edges[54].

In contrast to z_{11} and z_{22}, z_{111122} can achieve the maximum density of benzenoid rings without imposing unpaired electron on the edge (Figure 4c). Moreover, z_{111122} can be further stabilized by the conjugation interaction between edge C=C double bonds. It is known that generally conjugation stabilization is stronger than hyperconjugation stabilization[55,56]. As a result, z_{111122} favors the nonmagnetic ground state and has a lower E_{edge} than z_{11}. For z_{1122}, when the edge carbon atoms are all saturated, the inner carbon atoms can only be partially benzenoid (Figure 4d). However, imposing unpaired electron on edge cannot increase the number of benzenoid rings. Therefore, z_{1122} also favors the nonmagnetic ground state.

Finally, an interesting question arises: is pure sp^2 termination a guarantee for edge magnetism? Taking an example, like hydrogen and C_2H_4, C_2H_2 can only form single bonds with edge carbon atoms, and intuitively may not disturb the π electron system of *z*GNR. Then, is C_2H_2, the dehydrogenation product of C_2H_4, also an ideal terminal group for *z*GNRs?

To address this concern, we investigated two edge configurations for C_2H_2 terminated 8-*z*GNRs (8-C_2H_2-*z*GNR), including z_{11} and z_{111122}. In contrast to 8-C_2H_4-*z*GNR, z_{11} of 8-C_2H_2-*z*GNR (−0.205 eV/Å) has a lower E_{edge} than z_{111122} (−0.196 eV/Å). Moreover, our computations revealed that both z_{11} and z_{111122} of 8-C_2H_2-*z*GNR have a nonmagnetic ground state. At first glance, this is rather surprising. The nonmagnetic z_{111122} of 8-C_2H_2-*z*GNR can be understood in the same away as discussed above for 8-C_2H_4-*z*GNR. However, why is z_{11} of 8-C_2H_2-*z*GNR also nonmagnetic? This seemingly unexpected result can also be understood by the competition between hyperconjugation, conjugation and maximizing benzenoid rings.

In contrast to the general intuition, C_2H_2 terminations significantly differ from C_2H_4 terminations, since C_2H_2 can couple to the π electron system of *z*GNR by forming double bonds with edge sites in the dominant resonance structure (Figure 5a): in a 1×1×3 supercell of z_{11} of 8-C_2H_2-*z*GNR, two C_2H_2 molecules each form two C-C single bonds with two edge sites in each edge, but the third C_2H_2 molecule forms two C=C bonds with two edge sites. With the help of newly formed C=C bonds, the carbon atoms of 8-C_2H_2-*z*GNR can achieve a density of benzenoid rings of 2/7 without imposing unpaired electron on the edge.

We can also get the resonance structure (Figure 5b) by imposing two unpaired electrons on each edge, in which the density of benzenoid rings can be increased to the maximum (1/3), the same as z_{11} of 8-C_2H_4-*z*GNR. However, this magnetic state is not favorable

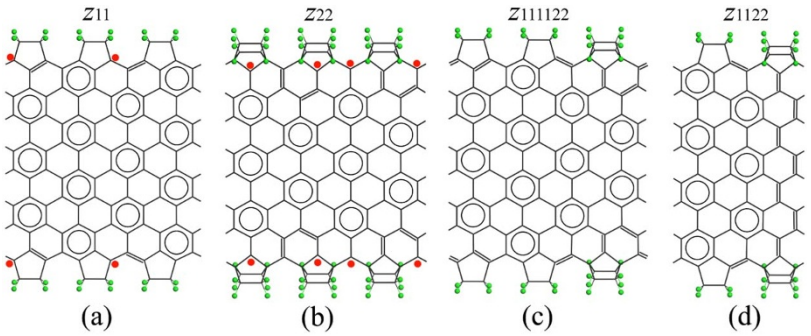

Figure 4 | Clar representations for 8-C_2H_4-*z*GNR with different edge configurations. (a) z_{11}, (b) z_{22}, (c) z_{111122}, and (d) z_{1122}. Doublet and circle denote C=C double bond and benzenoid ring, respectively. The red point represents unpaired electron.

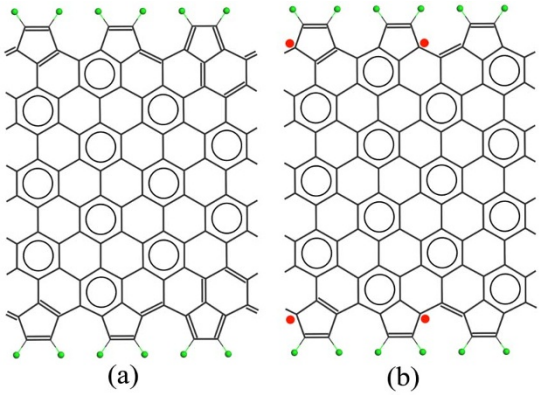

Figure 5 | Clar representations of 8-C_2H_2-*z*GNR in z_{11} edge configuration. (a) and (b) represent the nonmagnetic and magnetic states, respectively.

energetically since the conjugation in the nonmagnetic state overwhelms the energy gain by maximizing the benzenoid rings. In the nonmagnetic state, the C=C bonds at edges have conjugation interaction along the zigzag direction; in the magnetic state, there exists hyperconjugation interaction between unpaired electrons and neighboring C=C bonds. The much stronger conjugation stabilization in the nonmagnetic state over the hyperconjugation stabilization in the magnetic state overcompensates the unfavorability of the nonmagnetic state with fewer benzenoid rings, which leads to a nonmagnetic ground state.

Another question is why z_{11} 8-C_2H_2-*z*GNR has a lower E_{edge} than z_{111122}. Note that z_{111122} has the same density of benzenoid rings as z_{11}, and it also has the conjugation stabilization among edge C=C bonds (Figure S4 of supplementary information). However, the conjugation interaction in z_{111122} is not continuous in the zigzag direction while the conjugation interaction in z_{11} is continuous. Therefore, z_{111122} has a slightly lower E_{edge} than z_{11}.

Overall, though C_2H_2 termination can produce sp^2 coordinated edges with energetically very favorable E_{edge}, C_2H_2 can suppress the edge magnetism by coupling to the π-electron system of *z*GNR, which disqualifies C_2H_2 as an ideal terminal group for *z*GNRs. Therefore, even pure sp^2 termination is not a guarantee for edge magnetism.

To summarize, by means of DFT computations, we systemically studied the energetics and electronic properties of C_2H_4-*z*GNRs with different edge configurations. The pure sp^2 coordinated edges, namely z_{11}, can be stabilized at rather mild experimental conditions. Especially, such C_2H_4-*z*GNRs with sp^2 edges can well reproduce the magnetic and electronic properties of H-*z*GNRs. Therefore, C_2H_4 is an ideal terminal group for *z*GNRs in terms of preserving the edge magnetism. Interestingly, the edge electronic structures of C_2H_4-*z*GNRs can be well interpreted by employing the Clar's rule. Further analysis identified multiple hyperconjugation interactions as the key factor responsible for enhanced stability of the sp^2 coordinated edges. Moreover, we demonstrated that pure sp^2 termination can not guarantee edge magnetism for zGNRs, for example, C_2H_2 termination can couple to the π-electron system of *z*GNRs, and suppress the magnetism. These findings would deepen our basic knowledge of graphene electronics and provide a feasible way for realizing *z*GNR-based spintronics.

Methods

DFT computations were performed using the plane-wave technique implemented in Vienna *ab initio* simulation package (VASP)[57]. The ion-electron interaction is described using the projector-augmented plane wave (PAW) approach[58,59]. GGA expressed by PBE functional[60] and a 400 eV cutoff for the plane-wave basis set were adopted in all computations. Self-consistent field (SCF) calculations were conducted with a convergence criterion of 10^{-4} eV on the total energy and the electron density. 1D periodic boundary condition (PBC) was applied along the *z* direction in order to simulate their infinitely long systems. The minimum distance between two ribbons is larger than 15 Å, which can safely avoid the interaction between two ribbons. The Brillouin zone was sampled with a 1×1×10 Γ centered *k* points. Based on the optimized geometric structures, 21 *k*-points were used to obtain the band structures.

1. Novoselov, K. S. *et al.* Electric field effect in atomically thin carbon films. *Science* **306**, 666–669 (2004).
2. Novoselov, K. S. *et al.* Two-dimensional atomic crystals. *Proc. Natl. Acad. Sci. U.S.A.* **102**, 10451–10453 (2005).
3. Novoselov, K. S. *et al.* A roadmap for graphene. *Nature* **490**, 192–200 (2012).
4. Georgakilas, V. *et al.* Functionalization of graphene: covalent and non-covalent approaches, derivatives and applications. *Chem. Rev.* **112**, 6156–6214 (2012).
5. Tang, Q., Zhou, Z. & Chen, Z. F. Graphene-related nanomaterials: tuning properties by functionalization. *Nanoscale* **5**, 4541–4583 (2013).
6. Son, Y.-W., Cohen, M. L. & Louie, S. G. Energy gaps in graphene nanoribbons. *Phys. Rev. Lett.*, **97**, 216803 (2006).
7. Barone, V., Hod, O. & Scuseria, G. E. Electronic structure and stability of semiconducting graphene nanoribbons. *Nano Lett.* **6**, 2748–2754 (2006).
8. Li, X. L., Wang, X. R., Zhang, L., Lee, S. W. & Dai, H. J. Chemically derived, ultrasmooth graphene nanoribbon semiconductors. *Science* **319**, 1229–1232 (2008).
9. Han, M. Y., Özyilmaz, B., Zhang, Y. & Kim, P. Energy band-gap engineering of graphene nanoribbons. *Phys. Rev. Lett.* **98**, 206805 (2007).
10. Fujita, M., Wakabayashi, K., Nakada, K. & Kusakabe, K. Peculiar localized state at zigzag graphite edge. *J. Phys. Soc. Jpn.* **65**, 1920–1923 (1996).
11. Nakada, K., Fujita, M., Dresselhaus, G. & Dresselhaus, M. S. Edge state in graphene ribbons: nanometer size effect and edge shape dependence. *Phys. Rev. B* **54**, 17954–17961 (1996).
12. Wakabayashi, K., Sigrist, M. & Fujita, M. Spin wave mode of edge-localized magnetic states in nanographite zigzag ribbons. *J. Phys. Soc. Jpn.* **67**, 2089–2093 (1998).
13. Son, Y.-W., Cohen, M. L. & Louie, S. G. Half-metallic graphene nanoribbons. *Nature* **444**, 347–349 (2006).
14. Kan, E. J., Li, Z. Y., Yang, J. L. & Hou, J. G. Half-metallicity in edge-modified zigzag gaphene nanoribbons. *J. Am. Chem. Soc.* **130**, 4224–4225 (2008).
15. Li, Y. F., Zhou, Z., Shen, P. W. & Chen, Z. Spin gapless semiconductor-metal-half-metal properties in nitrogen-doped zigzag graphene nanoribbons. *ACS Nano*, **3**, 1952–1958 (2009).
16. Jiang, D. E., Sumpter, B. G. & Dai, S. Unique chemical reactivity of a graphene nanoribbon's zigzag edge. *J. Chem. Phys.* **126**, 134701 (2007).
17. Okada, S. Energetics of nanoscale graphene ribbons: edge geometries and electronic structures. *Phys. Rev. B* **77**, 041408 (2008).
18. Huang, B. *et al.* Quantum manifestations of graphene edge stress and edge instability: a first-principles study. *Phys. Rev. Lett.* **102**, 166404 (2009).
19. Koshinen, P., Malola, S. & Häkkinen, H. Self-passivating edge reconstructions of graphene. *Phys. Rev. Lett.* **101**, 115502 (2008).
20. Kastler, M., Schmidt, J., Pisula, W., Sebastiani, D. & Müllen, K. From armchair to zigzag peripheries in nanographenes. *J. Am. Chem. Soc.* **128**, 9526–9534 (2006).
21. Cai, J. M. *et al.* Atomically precise bottom-up fabrication of graphene nanoribbons. *Nature* **466**, 470–473 (2010).
22. Jiao, L. Y., Zhang, L., Wang, X. R., Diankov, G. & Dai, H. J. Narrow graphene nanoribbons from carbon nanotubes. *Nature* **458**, 877–880 (2009).
23. Kosynkin, D. V. *et al.* Longitudinal unzipping of carbon nanotubes to form graphene nanoribbons. *Nature* **458**, 872–876 (2009).
24. Jiao, L. Y., Wang, X. R., Diankov, G., Wang, H. & Dai, H. J. Facile synthesis of high-quality graphene nanoribbons. *Nature Nanotechnol.* **5**, 321–325 (2010).
25. Campos-Delgado, J. *et al.* Bulk production of a new form of sp^2 carbon: crystalline Ggraphene. *Nano Lett.* **8**, 2773–2778 (2008).
26. Morelos-Gómez, A. *et al.* Clean nanotube unzipping by abrupt thermal expansion of molecular nitrogen: graphene nanoribbons with atomically smooth edges. *ACS Nano.* **6**, 2261–2271 (2012).
27. Kobayashi, Y., Fukui, K., Enoki, T. & Kusakabe, K. Edge state on hydrogen-terminated graphite edges investigated by scanning tunneling microscopy, *Phys. Rev. B* **73**, 125415 (2006).
28. Riter, K. A. & Lyding, J. W. The influence of edge structure on the electronic properties of graphene quantum dots and nanoribbons. *Nat. Mater.* **8**, 235–242 (2009).
29. Tao, C. *et al.* Spatially resolving edge states of chiral graphene nanoribbons. *Nat. Phys.* **7**, 616–620 (2011).
30. Pan, M. *et al.* Topographic and spectroscopic characterization of electronic edge states in CVD grown graphene nanoribbons. *Nano Lett.* **12**, 1928–1933 (2012).
31. Zhang, X. *et al.* Experimentally engineering the edge termination of graphene nanoribbons. *ACS Nano.* **7**, 198–202 (2013).
32. Joseph Joly, V. L. *et al.* Observation of magnetic edge state in graphene nanoribbons. *Phys. Rev. B* **81**, 245428 (2010).
33. Konishi, A. *et al. J. Am. Chem. Soc.* **135**, 1430–1437 (2013).
34. Wassmann, T., Seitsonen, A. P., Saitta, A. M., Lazzeri, M. & Mauri, F. Structure, stability, edge states, and aromaticity of graphene ribbons. *Phys. Rev. Lett.* **101**, 096402 (2008).

35. Seitsonen, A. P., Saitta, A. M., Wassmann, T., Lazzeri, M. & Mauri, F. Structure and stability of graphene nanoribbons in oxygen, carbon dioxide, water, and ammonia. *Phys. Rev. B* **82**, 115425 (2010).
36. Chia, C.-I. & Crespi, V. H. Stabilizing the zigzag edge: graphene nanoribbons with sterically constrained terminations. *Phys. Rev. Lett.* **109**, 076802 (2012).
37. Plasser, F. *et al*. The multiradical character of one- and two-dimensional graphene nanoribbons. *Angew. Chem. Int. Ed.* **52**, 2581–2584 (2013).
38. Gao, L., Guest, J. R. & Guisinger, N. P. Epitaxial graphene on Cu(111). *Nano Lett.* **10**, 3512–3516 (2010).
39. Martinez-Galera, A., Brihuega, I. & Gómez-Rodríguez, J. M. Ethylene irradiation: a new route to grow graphene on low reactivity metals. *Nano Lett.* **11**, 3576–3580 (2011).
40. Koskinen, P., Malola, S. & Häkkinen, H. Evidence for Graphene Edges Beyond Zigzag and Armchair. *Phys. Rev B* **80**, 073401 (2009).
41. Lide, D. R. CRC Handbook of chemistry and physics. (CRC, Boca Raton, 2008).
42. Li, Y., Zhou, Z., Shen, P. & Chen, Z. Electronic and magnetic properties of hybrid graphene nanoribbons with zigzag-armchair heterojunctions. *J. Phys. Chem. C* **116**, 208–213 (2012).
43. Clar, E. Polycyclic hydrocarbons. (Academic Press: New York, 1964).
44. Clar, E. The aromatic sextet. (Wiley: London, 1972).
45. Watson, M. D., Fechtenkötter, A. & Müllen, K. Big is beautiful—"aromaticity" revisited from the viewpoint of macromolecular and supramolecular benzene chemistry. *Chem. Rev.* **101**, 1267–1300 (2001).
46. Randic, M. Aromaticity of polycyclic conjugated hydrocarbons. *Chem. Rev.* **103**, 3449–3606 (2003).
47. Popov, I. A. & Bolydrev, A. I. Chemical Bonding in Coronene, Isocoronene, and Circumcoronene. *Eur. J. Org. Chem.* 3485–3491 (2012).
48. Wassmann, T., Seitsonen, A. P., Saitta, A. M., Lazzeri, M. & Mauri, F. Clar's theory, π-electron sistribution, and deometry of graphene nanoribbons. *J. Am. Chem. Soc.* **132**, 3440–3451 (2010).
49. Gao, X. F., Zhao, Y. L., Liu, B., Xiang, H. J. & Zhang, S. B. π-bond maximization of graphene in hydrogen addition reactions. *Nanoscale.* **4**, 1171–1176 (2012).
50. Popov, I. A., Bozhenko, K. V. & Boldyrev, A. I. Is graphene aromatic? *Nano Res.* **5**, 117–123 (2012).
51. Popov, I. A. & Boldyrev, A. I. Deciphering chemical bonding in a BC_3 honeycomb epitaxial sheet. *J. Phys. Chem. C* **116**, 3147–3152 (2012).
52. Popov, I. A. & Boldyrev, A. I. Chemical bonding in coronene, isocoronene, and circumcoronene. *Eur. J. Org. Chem.* **2012**, 3485–3491 (2012).
53. Li, Y. & Chen, Z. Patterned partially hydrogenated graphene (C_4H) and its one-dimensional analogues: a computational study. *J. Phys. Chem. C.* **116**, 4526–4534 (2012).
54. Kudin, K. N. Zigzag graphene nanoribbons with saturated edges. *ACS Nano* **2**, 516–522 (2008).
55. Jarowski, P. D., Wodrich, M. D., Wannere, C. S., Schleyer, P. v. R. & Houk, K. N. How large is the conjugative stabilization of diynes? *J. Am. Chem. Soc.* **126**, 15036–15038 (2004).
56. Fernández, I. & Frenking, G. Direct estimate of the strength of conjugation and hyperconjugation by the energy decomposition analysis method. *Chem.–Eur. J.* **12**, 3617–3629 (2006).
57. Kresse, G. & Hafner, J. Ab initio molecular dynamics for liquid metals. *Phys. Rev. B* **47**, 558–561 (1993).
58. Blöchl, P. E. Projector augmented-wave method. *Phys. Rev B* **50**, 17953–17979 (1994).
59. Kresse, G. & Joubert, D. From ultrasoft pseudopotentials to the projector augmented-wave method. *Phys. Rev B* **59**, 1758–1775 (1999).
60. Perdew, J. P., Burke, L. & Ernzerhof, M. Generalized gradient approximation made simple. *Phys. Rev. Lett.* **77**, 3865–3868 (1996).

Acknowledgments

Support by Department of Defense (Grant W911NF-12-1-0083) and NSF (Grant EPS-1010094) in the US and the 111 Project (B12015) in China is gratefully acknowledged. CRC acknowledges the financial support of NSF NSEC Center for Hierarchical Manufacturing Grant No. CHM - CMMI – 0531171.

Author contributions

Z.C. conceived the initial idea of this research. Y.L. demonstrated the initial idea and collected all the data. Z.Z. and C.C. participated in the discussion. Y.L. and Z.C. drafted the paper, and all coauthors revised the manuscript. Z.C. guided the work.

Additional information

Supplementary information accompanies this paper at http://www.nature.com/scientificreports

Competing financial interests: The authors declare no competing financial interests.

How to cite this article: Li, Y., Zhou, Z., Cabrera, C.R. & Chen, Z. Preserving the Edge Magnetism of Zigzag Graphene Nanoribbons by Ethylene Termination: Insight by Clar's Rule. *Sci. Rep.* **3**, 2030; DOI:10.1038/srep02030 (2013).